CORE
Metadata, citation and similar papers at core.ac.uk
Provided by Explore Bristol Research

Lord, G. J., Champneys, A. R., & Hunt, G. W. (1997). The role of homoclinic bifurcations in understanding the buckling of long thin cylindrical shells.

Early version, also known as pre-print

Link to publication record in Explore Bristol Research
PDF-document

University of Bristol - Explore Bristol Research

General rights

This document is made available in accordance with publisher policies. Please cite only the published version using the reference above. Full terms of use are available:
http://www.bristol.ac.uk/pure/about/ebr-terms.html

THE ROLE OF HOMOCLINIC BIFURCATIONS IN UNDERSTANDING THE BUCKLING OF LONG THIN CYLINDRICAL SHELLS

G. J. LORD AND A. R. CHAMPNEYS
Department of Engineering Mathematics
University Walk, University of Bristol
Bristol, BS8 1TR, U.K.
G.J.Lord@bristol.ac.uk, A.R.Champneys@bristol.ac.uk

AND

G. W. HUNT
School of Mechanical Engineering
University of Bath, Bath, BA2 7AY, UK.
G.W.Hunt@bath.ac.uk

Abstract.

Experiments have shown that long cylinders buckle into localized patterns axially. It is argued that traditional linear or nonlinear analysis is unlikely to capture such modes, nor the effective buckling load at which such responses stabilise. However, the inherent translational indeterminacy of localised buckling is well captured by considering infinitely long cylinders and seeking homoclinic solutions of the von Kármán–Donnell equations. This exploits the dynamical analogy of such structural problems, so that symmetry arguments and numerical techniques developed for dynamical systems may be used. The method is illustrated by successful application to a cylinder which has well documented experimental results.

1. Introduction

A fruitful approach to certain statics problems posed over long domains has been to treat them as dynamical systems (see, for example, the contribution by J.M.T. Thompson in these proceedings). Localized responses of such systems, which energy arguments often reveal as being important

physically, may be modelled by homoclinic solutions of ordinary differential equations differential equations (ODEs) posed on the real line.

We aim to show succinctly that the buckling of long thin, cylindrical shells is a classically hard problem that is well explained using this approach. The equilibrium of the shell is governed by the von Kármán–Donnell partial differential equations (PDEs), which may be viewed as a dynamical system in the axial length of the cylinder. The difficulty for traditional analysis (using modal decomposition or finite element techniques) is that buckling is violently sub-critical, so that linear theory can over-predict the true experimentally observed load by as much as 400% (see, for example, Figure 1(a) where the true buckling load is near the turning point of the post-buckled curve). Therefore, the nature of post buckling behaviour is fundamental in predicting the true failure loads and displacements.

Figure 1 reproduces some experimental work from the 1970s depicting *elastic* buckling deformations of moderately long cylinders under end loading. Several features are worthy of note. First, buckling is typically localized to some portion of the axial length of the cylinder. Secondly, there is a translational indeterminacy axially in the location of the buckled portion (compare (c) and (d)). Thirdly, for each buckle there is a well defined circumferential 'wave number', which is *not* fixed by the geometry of the cylinder. Finally, there are two forms of buckle pattern (cf. Figure 1(b),(d)) which in the following we refer to as *symmetric* and *cross-symmetric* respectively.

In this paper we show how our numerical methods, based on the dynamical systems analogy, captures all the features of Von Eßlinger and Geier's experiments both qualitatively and quantitatively. We consider an infinitely long cylinder and discretize the von Kármán–Donnell equations circumferentially by a Galerkin method. This yields a large system of ODEs in the axial variable x, for which we seek homoclinic, i.e. axially localized, solutions. We seek forms of solutions which are either symmetric or cross-symmetric, implying reversibilities of the ODEs.

In earlier work (Lord, Champneys & Hunt 1997*a*, Lord, Champneys & Hunt 1997*b*), we confirmed numerically the existence of homoclinic orbit solutions to these equations and obtained good agreement with experimental data on a cylinder due to Yamaki (1984). We also described in detail the numerical techniques used to compute those solutions, which are based on extension to the current PDE setting of existing methods for homoclinic solutions or ODEs (e.g. (Beyn 1990, Friedman & Doedel 1994)). We are interested here in "primary" or "uni–modal" homoclinic orbits. However recent work by Peterhof, Sandstede & Scheel (1997) strongly suggests the existence of "multi–modal" or n-pulse homoclinic orbits such as computed in Lord et al. (1997*a*).

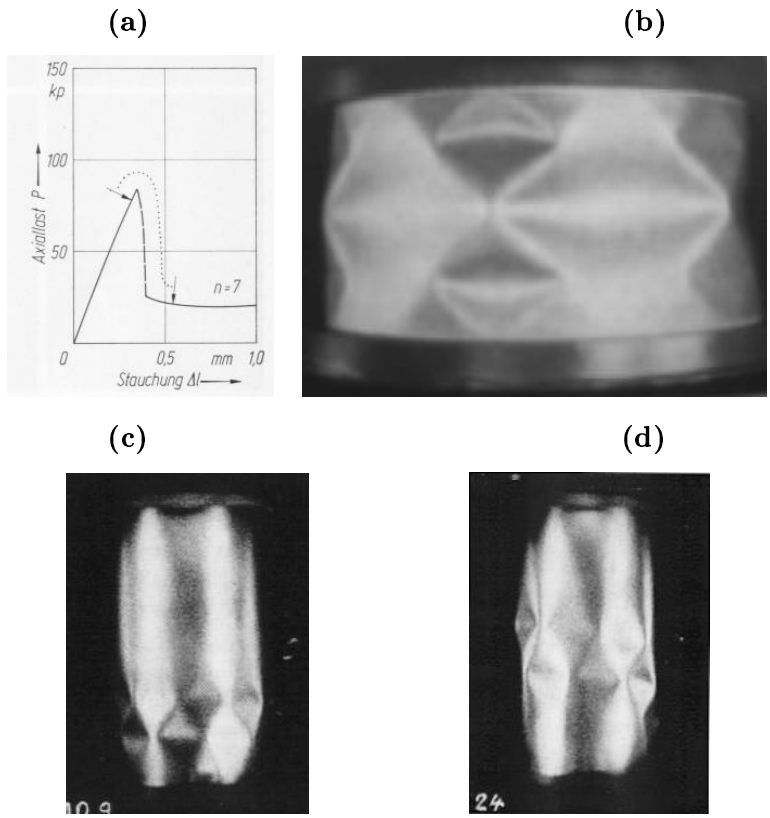

Figure 1. Experimental results after Von Eßlinger 1970 and Von Eßlinger & Geier 1972. (a) Load vs end-shortening bifurcation diagram taken from experiment (1970). (b) Symmetric solution found on a short cylinder (1972). (c) Cross-symmetric solution localized close to one end of cylinder (1970), and (d) cross-symmetric solution localized just off centre of cylinder(1970). In (b) and (d) we see an axial translation of the same buckle pattern.

In Section 2, we describe the von Kármán–Donnell equations, their Galerkin approximation and how to exploit symmetries in the problem. Section 3 then presents numerical results and compares them to the experiments. All our computations were performed using the numerical continuation code AUTO (Doedel, Keller & Kernévez 1991). Finally, Section 4 draws conclusions.

2. The von Kármán–Donnell equations and their approximation as a dynamical system

Consider an infinitely long, thin cylindrical shell of radius R and shell thickness t. The classical equilibrium equations for the in–plane stress function

ϕ and displacement w in the post–buckling regime of the cylinder are given by the von Kármán–Donnell equations:

$$\kappa^2\nabla^4 w + \lambda w_{xx} - \rho\phi_{xx} = w_{xx}\phi_{yy} + w_{yy}\phi_{xx} - 2w_{xy}\phi_{xy} \tag{1}$$

$$\nabla^4\phi + \rho w_{xx} = (w_{xy})^2 - w_{xx}w_{yy}, \tag{2}$$

where ∇^4 denotes the two dimensional bi–harmonic operator; $x \in \mathbb{R}$ is the axial and $y \in [0, 2\pi R)$ is the circumferential co-ordinate. The parameters appearing in (1) and (2) are the curvature $\rho := 1/R$, $\kappa^2 := t^2/12(1-\nu^2)$, where ν is Poisson's ratio, and the load parameter $\lambda := P/Et$, where P is the compressive axial load (force per unit length) and E is Young's modulus. The form of solutions we seek suggest that equations (1) and (2) should be supplemented with periodic boundary conditions in y and asymptotic boundary conditions in the axial direction x:

$$\begin{gathered}(w,\phi)(x,0) = (w,\phi)(x,2\pi R),\\ (w,\phi)(x,y), (w,\phi)_x(x,y), (w,\phi)_{xx}(x,y), (w,\phi)_{xxx}(x,y) \to 0 \text{ as } \ x \to \pm\infty.\end{gathered} \tag{3}$$

The system (1) and (2) has a rich structure of symmetries, see (Hunt, Williams & Cowell 1986, Wohlever & Healey 1995). In accordance with observed deformation patterns, we seek solutions that are even periodic solutions in y and which remain within the subspace corresponding to invariance under rotation through $2\pi/s$. Hence we use the following cosine functions as the basis functions in the Galerkin approximation

$$w(y) = \sum_{m=0}^{\infty} a_m \cos(ms\rho y); \qquad \phi(y) = \sum_{m=0}^{\infty} b_m \cos(ms\rho y), \qquad s \in \mathbb{N}.$$

We refer to $\cos(s\rho y)$ as the *seed mode*.

Substituting into the von Kármán–Donnell equations, taking the L^2 inner product and expanding the nonlinear terms we find a system of ODEs for the Fourier modes a_m and b_m for $m = 0, \ldots, \infty$ which we may formally write as

$$a_m^{iv} = La_m + F_m(a_m), \qquad b_m^{iv} = Lb_m + F_m(b_m), \tag{4}$$

where superscripts denote differentiation with respect to x (see (Lord et al. 1997*a*) for the details). The Galerkin approximation is formed by taking equations (4) for $m = 0, \cdots, M-1$, for some finite M.

We think of equations (4) as a dynamical system, with the axial variable x taking a time-like role. Systems of the form (4), arising from elliptic PDEs, were considered in detail by Mielke (1991), and shown to have a Hamiltonian structure.

There is a further symmetry of von Kármán–Donnell equations that plays an important role in the localised buckling solutions observed physically. The buckling modes observed experimentally, tend to be either *symmetric* (as in Figure 1(b)) or *cross-symmetric* (Figure 2(d)) about a horizontal cross-section of the cylinder. A solution to (1), (2) that is *symmetric* about the cross-section $x = T$ satisfies

$$w(x,y) = w(2T - x, y) \qquad \& \qquad \phi(x,y) = \phi(2T - x, y). \tag{5}$$

Equations (5) impose the natural symmetric conditions on the Fourier modes a_m and b_m for $m = 0, \cdots, M-1$ at $x = T$,

$$a_m'(T) = a_m''(T) = b_m'(T) = b_m''(T) = 0. \tag{6}$$

In contrast, a *cross-symmetric* solution satisfies, for some seed mode s,

$$w\left(x,y\right) = w\left(2T - x, y + \pi R/s\right) \ \& \ \phi\left(x,y\right) = \phi\left(2T - x, y + \pi R/s\right). \tag{7}$$

Thus, in terms of the Fourier modes, we have that

$$\begin{array}{ll} a_m'(T) = b_m'(T) = a_m'''(T) = b_m'''(T) = 0, & m = 0, 2, 4, \cdots; \\ a_m(T) = b_m(T) = a_m''(T) = b_m''(T) = 0, & m = 1, 3, 5, \cdots. \end{array} \tag{8}$$

It is not difficult to see that the symmetries of (1) and (2) defined by (5) and (7) define a *reversibility* of the ODEs (4), as in (Devaney 1976), with fixed point sets, S, forming $4M$–dimensional sub–manifolds of phase space $\mathbb{R}^{8M}$. Hence we can use as a boundary condition that the solution $a_m(T)$, $b_m(T)$, lie in the the $4M$–dimensional space S.

Note, finally, that there is a "degeneracy" in equations (4) for the zero mode ($m = 0$) such that these could be solved with initial conditions for $a_0'', a_0''', b_0'', b_0'''$ independently of the initial conditions for a_0, b_0 and a_0', and b_0'. This corresponds to a trivial translational symmetry in the problem (sometimes termed a rigid body mode). This translation invariance plays an important role. In our formulation the localization may occur at any point along the length of the cylinder. Indeed this translation invariance is observed experimentally (see for example Figures 3 and 4 in Von Eßlinger (1970), reproduced partially in Figure 1.

A standard periodic analysis of the von Kármán–Donnell equations seeks the minimum load $\lambda = \lambda_d$ and corresponding axial and circumferential wavelengths such that a bifurcation occurs. One may easily show in this way that $\lambda_d = 2\rho\kappa$. Wavelengths for which $\lambda = \lambda_d$ lie on a circle in axial/circumferential wave space as first elucidated by Koiter (1945). The weakly nonlinear analysis of Hunt & Lucena Neto (1991), interpreted in the present context, suggests that once a circumferential wave number has

been chosen, then there is a small amplitude bifurcation of (a pair of) homoclinic solutions at $\lambda = \lambda_d$ as in the normal form of a Hamiltonian-Hopf bifurcation (Iooss & Peroueme 1993).

In order to compute the true localised buckling load, we numerically extend the weakly nonlinear analysis, by computing homoclinic solutions to (4) truncated for some M. Note that the single mode approximation found by taking $M = 1$ ($m = 0$ only) in (4) yields a linear system for which there are no homoclinic solutions. Thus the simplest approximation we can take that may admit a homoclinic solution is the two mode approximation found by taking $M = 2$ ($m = 0, 1$) in (4).

The numerical method, described in detail in Lord et al. (1997*a*), makes full use of the reversibility and symmetry properties of (4) regarded as a dynamical system. Specifically, we solve for symmetric or cross-symmetric homoclinic solutions as a boundary-value problem (BVP) on a truncated domain, with left-hand projection boundary conditions that place the solution in the linearised unstable manifold of the origin (see, e.g. (Beyn 1990)). At the right-hand boundary conditions, we exploit the symmetric section conditions (6), (8). This BVP can be solved by a regular continuation code to compute load-deflection bifurcation diagrams, but may require careful steps to be taken in order to compute initial approximations.

3. Numerical results

To compare with the experiments of Von Eßlinger & Geier (1972) calculations were performed for a shell with

$$\rho = 0.01\text{mm}^{-1}, \qquad t = 0.190\text{mm}, \qquad \nu = 0.3, \qquad E = 4.11 \text{ GPa}. \quad (9)$$

In the figures below x is plotted on [0,2T] unless otherwise indicated and x,y,$w(x, y)$ and Fourier coefficients a_k are measured in *mm*. All computations were performed using the numerical continuation code AUTO (Doedel et al. 1991) and, unless otherwise stated, the number of collocation intervals NTST=20.

Note that the shell we compare to here is of length $L = 100$ mm and so hardly qualifies as long as its aspect ratio (length to diameter) is only $L/2R = 0.5$.

We compare with experiments the ratio of loads λ_m/λ_d where $\lambda_d = 2\rho\kappa \approx 1.1499 \times 10^{-3}$ denotes the smallest value of λ at which the fundamental solution bifurcates, and λ_m is the minimum post buckling load (the first local minimum in the bifurcation diagram, see Figures 2 & 3 (a)). For the numerical simulations, λ_m was taken to be the first limit point on the branch of homoclinics as the loading parameter was decreased from λ_d.

In the computations the half length of the cylinder T was taken to be either $T = 100$ or $T = 250$. We chose a 6 mode approximation (ie

$m = 0, 1, 2, 3, 4, 5)$ since it was found in (Lord et al. 1997*a*) that gave a good compromise between spatial convergence and tractability of the problem.

In the bifurcation diagrams, Figure 2 (a) and Figure 3(a), we plot the load λ against a measure of the end shortening defined by arc–length for a symmetric case and a cross-symmetric case. Note that the trivial branch (corresponding to the diagonal line in Figure 1 (a) is equivalent to the λ-axis here - since the von Kármán–Donnell equations factor out the overall squash of the cylinder. The curve of homoclinic orbits originates, in both cases, from the bifurcation point $\lambda_d \approx 1.1499 \times 10^{-3}$ on the λ axis. The limit point λ_m is at the first minimum value of the loading parameter λ along the curve originating at λ_d.

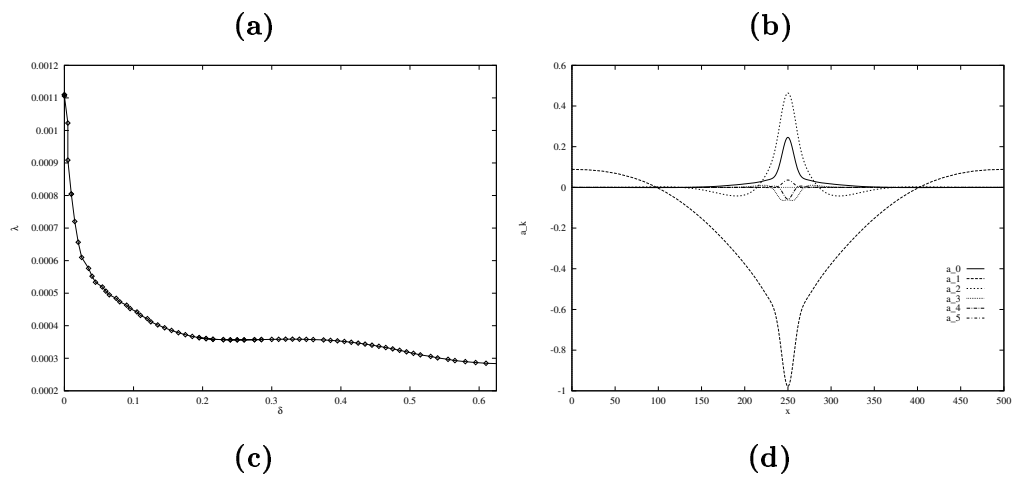

Figure 2. Symmetric form of solution computed for seed $s = 7$ with $M = 6$ modes. (a) Bifurcation diagram, (b) Fourier modes a_k (mm) for displacement, (c) reconstructed displacement w (mm), (d) reconstructed stress function ϕ.

In Figures 2 and 3 (b) we have plotted the Fourier modes a_k for the displacement w for the symmetric and cross symmetric cases respectively.

Note that the Fourier modes a_4 and a_5 are very small - indicating convergence as the spatial resolution is increased.

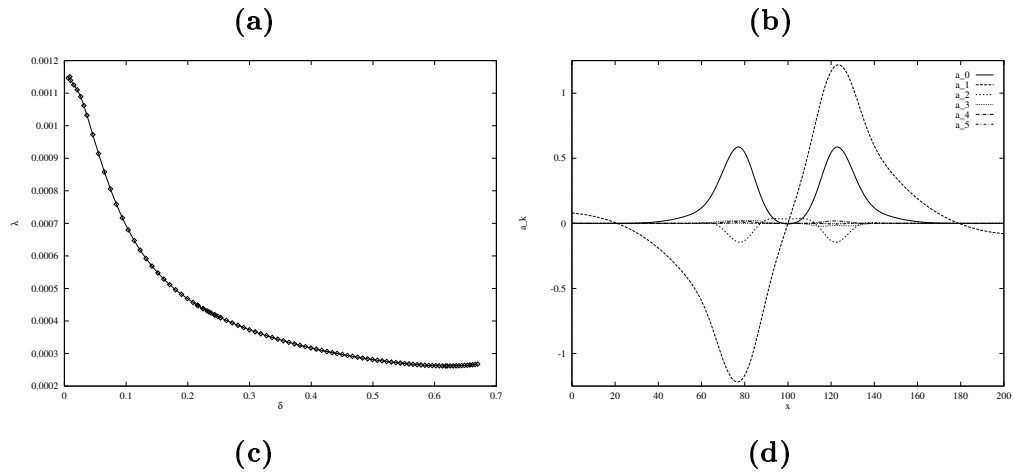

Figure 3. Cross-symmetric form of solution computed for seed $s = 7$ with $M = 6$ modes. (a) Bifurcation diagram, (b) Fourier modes a_m (mm) for displacement, (c) reconstructed displacement w (mm), (d) reconstructed stress function ϕ.

The 3-dimensional plot in Figures 2 and 3 (c) show the full reconstructed displacement $w(x, y)$ plotted over the deformed cylinder. The (cross-) symmetric nature of the solutions is clearly evident. Qualitatively, all the 3-dimensional plots compare well with the experimental evidence of Von Eßlinger & Geier (1972). In Figures 2 and 3 (d) we have reconstructed the stress function ϕ and plotted that over the deformed cylinder.

We now consider a quantative comparison between our numerics and experimental results. For the symmetric case we found a difference of $\approx$ 20% in the experimental to computed ratio λ_m/λ_d. This discrepancy is discussed below. In the cross-symmetric case excellent quantative agreement was obtained, as presented in Table 1.

s	10	11	12	13
Present	0.1843	0.2027	0.2277	0.2538
Experimental	0.197	0.208	0.228	0.257

TABLE 1. Comparison of the ratio λ_m/λ_d of our results with the experiments of Von Eßlinger & Geier (1972) for cross-symmetric forms of the solution.

4. Conclusion

We presented numerical results for the buckling cylinder problem and compared our results with experimental data. Qualitatively, we find good agreement for both the symmetric and cross-symmetric forms of solutions.

In the symmetric case there are some discrepancies between the numerical and experimental results. However, the experiments of Von Eßlinger & Geier (1972) indicate that a symmetric buckle pattern is not observed in longer cylinders. In addition, for the relatively short cylinder presented here, they find that the symmetric modes occur at lower-post buckling loads. This evidence is corroborated in (Yamaki 1984) who finds mostly cross-symmetric solutions. Furthermore symmetric modes appear less localized than cross-symmetric, and we would therefore not expect our analysis on this relatively short cylinder to be as quantatively accurate. For longer cylinders, for which there is little experimental evidence of the symmetric pattern, we would expect better agreement.

For the cross-symmetric case, more commonly observed experimentally, we have found excellent agreement quantatively even for the relatively short cylinder. For longer cylinders we expect a yet closer match to the experiments.

Our results suggest that the buckling of a long thin axially compressed cylinder is well described by a localization theory based on homoclinic solutions, independently of any imperfections in the cylinder. Significantly, this allows for the translational indeterminacy inherent in observations (cf. Figure 1). As such, we claim, it is provides a useful complement to finite element approaches with realistic boundary conditions, which may suffer from multiplicities of (near) solutions. This demonstrates that the corresponding asymptotic boundary conditions are the natural boundary conditions for the computation of buckling solutions of long cylinders.

References

Beyn, W.-J. (1990), 'The numerical computation of connecting orbits in dynamical systems', *IMA Journal of Numerical Analysis* **9**, 379–405.

Devaney, R. (1976), 'Reversible diffeomorphisms and flows', *Trans. Amer. Math. Soc.* (218), 89–113.

Doedel, E., Keller, H. & Kernévez, J. (1991), 'Numerical analysis and control of bifurcation problems', *Int. J. Bifurcation and Chaos* **1**, 493–520, 745–772.

Friedman, M. & Doedel, E. (1994), 'Numerical computational of invariant manifolds connecting fixed points.', *SIAM J. Num. Anal.* **28**, 789—808.

Hunt, G. W. & Lucena Neto, E. (1991), 'Localized buckling in long axially–loaded cylindrical shells', *J. Mech. Phys. Solids* **39**(7), 881–894.

Hunt, G. W., Williams, K. A. J. & Cowell, R. G. (1986), 'Hidden symmetry concepts in the elastic buckling of axially loaded cylinders', *Int. J. Solids Structures* **22**(12), 1501–1515.

Iooss, G. & Peroueme, M. C. (1993), 'Perturbed homoclinic solutions in reversible 1:1 resonance vector fields', *J. Diff. Eq.* **102**, 62–88.

Koiter, W. T. (1945), On the Stability of Elastic Equilibrium, PhD thesis, University of Delft. English Translation: Tech. Rep. AFFDL-TR-70-25 Air Force Flight Dyn. Lab. 1970.

Lord, G. J., Champneys, A. R. & Hunt, G. W. (1997*a*), Computation of homoclinic orbits in partial differential equations: An application to cylindrical shell buckling, Technical Report ANM Report 6.97, University of Bristol, Department of Engineering Mathematics, University of Bristol, BS8 1TR, UK. Submitted to SIAM J. Sci. Comp.

Lord, G. J., Champneys, A. R. & Hunt, G. W. (1997*b*), Computation of localized post buckling in long axially–compressed cylindrical shells, *in* A. R. Champneys, G. W. Hunt & M. Thompson, eds, 'Phil. Trans. Localization and Solitary Waves in Solid Mechanics', Royal Society.

Mielke, A. (1991), *Hamiltonian and Lagrangian flows on center manifolds: with applications to elliptic variational problems*, Lecture notes in mathematics; 1489, Springer-Verlag, Berlin.

Peterhof, D., Sandstede, B. & Scheel, A. (1997), 'Exponential dichotomies for solitary–wave solutions of semilinear elliptic equations on infinite cylinders', *J. Diff. Equ.* To Appear.

Von Eßlinger, M. (1970), 'Hochgeschwindigkeitsaufnahmen vom Beulvorgang dünnwandiger, axialbelasteter Zylinder', *Der Stahlbau* **3**, 73–76.

Von Eßlinger, M. & Geier, B. (1972), 'Gerechnete Nachbeullasten als untere Grenze der experimentallen axialen Beullasten von Kreiszylindern', *Der Stahlbau* **12**, 353–359.

Wohlever, J. & Healey, T. (1995), 'A group theoretic approach to the global- bifurcation analysis of an axially compressed cylindrical-shell', *Computer Methods in Applied Mechanics and Engineering* **122**, 315–349.

Yamaki, N. (1984), *Elastic Stability of Circular Cylindrical Shells*, Vol. 27 of *Applied Mathematics and Mechanics*, Elsevier.